Analytica Chimica Acta 1161 (2021) 338468

Contents lists available at ScienceDirect

Analytica Chimica Acta

journal homepage: www.elsevier.com/locate/aca

A silicon nitride ISFET based immunosensor for tumor necrosis factor-alpha detection in saliva. A promising tool for heart failure monitoring

Hamdi Ben Halima [a], Francesca G. Bellagambi [a, **], Albert Alcacer [b], Norman Pfeiffer [c], Albert Heuberger [d], Marie Hangouët [e], Nadia Zine [a], Joan Bausells [b], Abdelhamid Elaissari [a], Abdelhamid Errachid [a, *]

[a] Institute of Analytical Sciences (ISA) – UMR 5280, Claude Bernard Lyon 1 University, 69100, Villeurbanne, Lyon, France
[b] Institute of Microelectronics of Barcelona (IMB–CNM, CSIC), Campus UAB, 08193, Bellaterra, Barcelona, Spain
[c] Fraunhofer IIS, Fraunhofer Institute for Integrated Circuits, Am Wolfsmantel 33, 91058, Erlangen, Germany
[d] Information Technology (LIKE), Friedrich-Alexander-Universität Erlangen-Nürnberg (FAU), Am Wolfsmantel 33, 91058, Erlangen, Germany
[e] Institute of Analytical Sciences (ISA) – UMR 5280, French National Centre for Scientific Research (CNRS), 69100, Villeurbanne, Lyon, France

HIGHLIGHTS

- Antibody-functionalization of ion-sensitive field effect transistor (ISFET) for tumor necrosis factor-α detection in saliva.
- Electrochemical impedance spectroscopy for tumor necrosis factor-α quantification.
- Heart failure monitoring by saliva analysis.

GRAPHICAL ABSTRACT

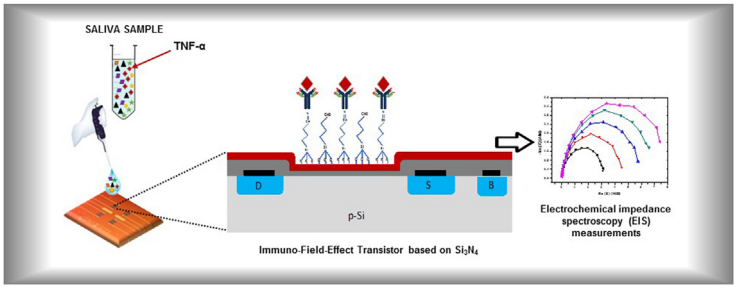

ARTICLE INFO

Article history:
Received 15 January 2021
Received in revised form
15 March 2021
Accepted 29 March 2021
Available online 2 April 2021

Keywords:
Biosensor
ImmunoFET
Tumor necrosis factor-α
Saliva analysis
Electrochemical impedance spectroscopy
Heart failure

ABSTRACT

According to the European statistics, approximately 26 million patients worldwide suffer from heart failure (HF), and this number seems to be steadily increasing. Inflammation plays a central role in the development of HF, and the pro-inflammatory cytokine Tumor necrosis factor-α (TNF-α) represents inflammation gold-standard biomarker. Early detection plays a crucial role for the prognosis and treatment of HF. An Ion Sensitive Field Effect Transistor (ISFET) based on silicon nitride transducer and bio-functionalized with anti-TNF-α antibody for label-free detection of salivary TNF-α is proposed. Electrochemical impedance spectroscopy (EIS) was used for TNF-α detection. Our ImmunoFET offered a detection limit of 1 pg mL^{-1}, with an analytical reproducibility expressed by a coefficient of variance (CV) resulted < 10% for the analysis of saliva samples, and an analyte recovery of 94 ± 6%. In addition, it demonstrated high selectivity when compared to other HF biomarkers such as Inteleukin-10, N-terminal pro B-type natriuretic peptide, and Cortisol. Finally, ImmunoFET accuracy in determining the unknown concentration of TNF-α was successfully tested in saliva samples by performing standard addition method. The proposed ImmunoFET showed great promise as a complementary tool for biomedical application for HF monitoring by a non-invasive, rapid and accurate assessment of TNF-α.

* Corresponding author.
** Corresponding author.
E-mail addresses: francesca.bellagambi@univ-lyon1.fr (F.G. Bellagambi), abdelhamid.errachid-el-salhi@univ-lyon1.fr (A. Errachid).

https://doi.org/10.1016/j.aca.2021.338468
0003-2670/

1. Introduction

Heart failure (HF) is a complex clinical syndrome caused by a wide range of cardiovascular disorders, such as structural or functional abnormalities of the heart, which results in the impairment of the heart ability to fill or to pump out blood may eventually lead to the clinical syndrome of HF. This cardiovascular chronic disease is currently the main cause of mortality and poor quality of life in western societies, affecting approximately 26 million people worldwide, and its prevalence continues to rise over time, with aging of the population [1,2].

Since HF imposes both direct costs to healthcare systems and indirect costs to society through morbidity, unpaid care costs, premature mortality and lost productivity, the estimation of global economic burden of HF is not accurately feasible. Therefore, increase of the population prone to HF requires a more specific and focused attention to both diagnosis and monitoring of the disease, both in the interest of patients than in the better management of costs linked to the spread of this disease [3,4]. In addition, patients with HF often present with signs and symptoms that are often nonspecific and with a wide differential diagnosis, making diagnosis by clinical presentation alone challenging that, unfortunately, can often result in delays in definitive diagnosis and treatment, and such delays are linked with poor prognosis [5]. Therefore, additional tools to aid clinical assessment would result helpful in making an accurate and prompt diagnosis, and effectively prognosticate, treat and better identify high-risk subjects [6]. The detection of specific biomarkers, which are measurable biological markers of a pathological process, provides information about variety biological conditions whether normal or pathological, and they can also be exploited not only to diagnose HF, but also to monitor the course of the therapy [7]. Among the established HF biomarkers, a raised circulating level of several inflammatory cytokines has been observed due to systemic inflammation that characterizes HF patients [8–10]. In particular, Tumor necrosis factor-alpha (TNF-α) is a pro-inflammatory cytokine observed following cardiac stress and whose dysregulation and excessive production were demonstrated implicated in the pathogenesis of HF as well as to adverse effects on other organs and apparatus, as well as on coagulation and immune system [11–13]. TNF-α is usually quantified in blood or plasma representing an additional stress, especially for elderly. Its concentration in healthy human plasma is usually less than 40 pg mL^{-1} [14,15], but its level increases up to hundreds according to HF severity [16,17]. TNF-α quantification is usually carried out in blood and by immunochemical methods, which provide accurate and provide rapid screening and multiple analyses, but several disadvantages also due to their high cost, the requirement of qualified personnel, and no possibility for real time measurement. For these reasons, biosensors are a very promising alternative due to their easy to use, reduced cost, portability, and possibility of on-line monitoring of biomarkers by in-situ measurements [18–20]. At the same time, the concentration of TNF-α in serum is reflected by its salivary levels [21] making TNF-α an ideal salivary biomarker for HF monitoring. The interest to use saliva as target matrix is due to the several offers advantages offered by saliva analysis if compared to blood: an easier and unobtrusively sampling (even from critical subjects such as children, elder and disabled people), the suitability for the screening of a large population by passing several drawbacks such as invasiveness and psychological stress (especially if repeated sampling is needed), and less health risks for patients and healthcare professionals [15,22–25].

In this paper we presented the development of an Ion Sensitive Field Effect Transistor (ISFET) based on silicon nitride transducer (Si_3N_4) and biofunctionalized for TNF-α detection in saliva for HF monitoring. For this purpose, monoclonal antibody TNF-α (mAb anti-TNF-α) were addressed onto the Si_3N_4 surface through covalent bonding of the aldehyde-silane (11-(triethoxysilyl) undecanal) TESUD obtaining an ImmunoFET. Our device provided a linear response and an adequate sensitivity for the target concentration range. Moreover, ImmunoFET selectivity was proven by analyzing samples containing three other HF biomarkers such as Inteleukin-10 (IL-10), N-terminal pro B-type natriuretic peptide (NT-proBNP), and Cortisol. Matrix effect was also properly investigated. Finally, the developed ImmunoFET was used to quantify TNF-α in real saliva samples by performing the standard addition method (STAM). Satisfactory results, proven by a mean accuracy of 98%, confirmed that our ImmunoFET can represent a promising tool for TNF-α monitoring in saliva for HF monitoring. Even if some papers already report the development of electrochemical sensors or biosensors for salivary TNF-α detection [19,20,26], our device would offer an innovative and promising approach based on the first time use of ISFET as sensing transducer combined with electrochemical impedance spectroscopy (EIS) for saliva sample analysis.

2. Materials and methods

2.1. Chemicals and reagents

TNF-α (Cat. No. 210-TA), mAb anti-TNF-α (Cat. No. MAB610), IL−10 (Cat. No. 1064-IL), sterile phosphate buffer saline solution (PBS) and PBS containing 0.1% bovine serum albumin (Cat. No. RB01 and RB02, respectively) were from R&D Systems (BioTechne, France). Hydrocortisone (cortisol, purity 99%, Cat. No. ab141250) was from abcam (France). NT-proBNP (Cat. No. 8NT2) was from HyTest (Finland). Millipore Milli-Q nanopure water (resistivity > 18 MΩ cm) was produced by a Millipore Reagent Water System (France). 11-triethoxysilyl undecanal (TESUD, 90%) was purchased from abcr (Germany). Pure ethanol (purity 95.0%) and sterile phosphate buffer saline (PBS) tablets were purchased from Sigma-Aldrich (France). PBS buffer used in this study was prepared by dissolving PBS tablets in the nanopure water as indicated by the supplier by yielding 0.01 M phosphate buffer (pH 7.4) containing 0.0027 M potassium chloride and 0.137 M sodium chloride. Epoxy resin EPO TEK H70E2LC was from Epoxy Technology (France).

2.2. Instrumentation

Wire bonding was performed using Kulicke & Soffa 4523 A Digital instrument from Kulicke & Soffa (Singapore). The UV/Ozone Procleaner™ (BioForce, Germany) was used in order to activate the ISFET's surface by creating −OH groups. The electrochemical measurements were performed using a VMP3 multichannel potentiostat purchased from Biologic-EC-Lab (France). Data acquisition and analysis were accomplished using EC-Lab software V11.30.

2.3. ISFET bio-functionalization

Microelectronic fabrication process for ISFET realization has been carried out at the National Microelectronics Centre (CSIC) of Institute of Microelectronics of Barcelona and it is described elsewhere [27]. ISFETs were bio-functionalized by the immobilization of mAb anti-TNF-α onto the ISFETs surface.

mAb anti-TNF-α have been diluted at 0.5 mg mL^{-1} in RB01 buffer according the procedure provided from the supplier. This stock solution was subsequently aliquoted and then stored at −20 °C until use. The 10 μg mL^{-1} mAb anti-TNF-α standard solution needed for ISFET functionalization has been obtained by further dilution of mAb mother solution in RB01 after gentle defrosting at 4 °C for 15 min before use.

The bio-functionalization process was started by cleaning the ISFETs with acetone/ethanol using sonicator bath; ISFETs were then thoroughly rinsed with Milli-Q water. Afterwards, the device was then placed for 30 min into the UV/O_3 cleaner to activate ISFET surface by creating −OH groups onto the Si_3N_4 surface. Subsequently, the activated ISFETs were functionalized with TESUD ((11-triethoxysilyl) undecanal) using vapor-phase method, an activation process already presented by our group in which Si_3N_4 and HfO_2 surfaces have been aldehyde-functionalized to detect human serum albumin [28] and salivary cortisol [29], respectively.

Then, the devices were placed into an oven at 100 °C for 1 h. After that, ISFETs were rinsed with absolute ethanol and dried using nitrogen to eliminate the excess of TESUD. Next, the functionalized ISFETs were incubated with mAb anti-TNF-α (10 μg mL^{-1} in PBS). Finally, the ImmunoFET was left in ethanolamine (1% v/v in PBS) for 45 min at room temperature (20 ± 2 °C). This step was very important to prevent nonspecific bonding at the detection stage.

2.4. Standard solutions and saliva samples preparation

TNF-α have been reconstituted at 0.1 mg mL^{-1} in RB02 buffer according to the reconstitution procedure provided from the supplier. This stock solution was then aliquoted and stored at −20 °C until use. Before use, each aliquot (10 μL) was gently defrosted at 4 °C for 15 min and then it was further diluted in PBS to obtain working standard solutions needed for both calibrations in PBS (in the concentration range 1–50 pg mL^{-1}) and for spiking saliva samples.

Standard solutions containing other HF biomarkers in PBS (e.g. IL-10, NT-proBNP, and cortisol, in the concentration range 5–20 pg mL^{-1}) have been prepared in a similar way to carry out the interference study.

Saliva has been collected from nominally healthy volunteers according to a procedure described elsewhere [23,30]. Briefly, subjects were asked to freely roll a synthetic swab (Salivette® from Sarstedt, Germany) in their mouth. Saliva was then recovered by centrifugation of the swab at 7000 rpm for 5 min at 4 °C, and all samples were pooled. The pooled saliva sample (PSS) was then aliquoted.

One aliquot (5 mL) was used for preparing calibration samples (TNF-α calibration in saliva) to investigate both method linearity and matrix effect. Matrix effect was excluded by comparing, at a confidence level of 95%, the slopes, reported with the corresponding standard deviation, of the calibration curves obtained by analyzing TNF-α standard solutions in PBS and saliva samples spiked in the same concentration range [31].

Another aliquot (450 μL) was analyzed by performing the STAM. To confirm the result, two other aliquots (450 μL) were spiked with a known amount of TNF-α to obtain two samples containing 50 and 330 pg mL^{-1} respectively. These samples have been treated as *unknown samples* and analyzed by carrying out the STAM.

STAM samples were prepared by adding a constant volume (50 μL) of sample to each of four 1.5 mL Eppendorf® Lo-bind centrifuge tubes (Eppendorf, France). The first tube was then made up to a final volume of 1 mL by adding 950 μL of PBS, obtaining the sample C_0. Increasing volumes of a 500 ng mL^{-1} TNF-α standard solution were added to the subsequent tubes and each flask was then made up to 1 mL with PBS, obtaining sample C_1 (addition of 20 pg mL^{-1}), sample C_2 (addition of 50 pg mL^{-1}), and sample C_3 (addition of 100 pg mL^{-1}), respectively. Afterwards, SAM samples were analyzed by EIS as described in 2.5.

2.5. EIS measurements

EIS measurements have been carried out after incubation at room temperature (20 ± 2 °C) of the ImmunoFET in standard solutions, spiked saliva samples or STAM samples for 30 min each, followed by PBS washing. EIS measurements were carried out in PBS, with a frequency ranged from 10 kHz to 10 Hz, two frequency points per frequency decade, and using a modulation voltage of 75 mV (E_{ac}). During the measurements, the potential was kept at 0 V (E_{dc}) versus the Ag/AgCl referenceEIS measurements were performed at room temperature (20 ± 2 °C) and in a faraday cage to avoid electrical and luminosity interference. The modeling of the obtained EIS data was achieved by the EC-Lab software using the Randomize + Simplex method, stopped on 5000 iterations.

Data fitting on EIS spectra was achieved using an equivalent circuit model [$R_1 + Q_2/R_2$] shown in Fig. 1, in which $R_1 = R_s$ and it corresponds to the resistance of the electrolyte solution (PBS); Q_2 is the constant phase element (CPE) that is in parallel with R_2, which is the charge transfer resistance (R_{ct}). Curves were obtained by plotting the ΔR/R normalized data as a function of TNF-α concentration. ΔR/R values have been normalized using the following equation $(R_{Ag} - R_{Ab})/R_{Ab}$, where R_{Ag} corresponds to R_2 of the antigen (TNF-α), and R_{Ab} to the R_2 of mAb anti-TNF-α.

3. Results and discussion

3.1. Standard solution analysis

Our ImmunoFET was first tested to verify the interaction between immobilized mAb anti-TNF-α and recombinant human TNF-α in the concentration range from 1 to 50 pg mL^{-1}. This concentration range was chosen taking into account both the dilution factor of 20 provided for STAM sample preparation and the TNF-α concentration range expected in saliva collected from HF patients (from few dozen up to 1000 pg mL^{-1}). Fig .1A shows the Nyquist plots obtained by plotting the real part of impedance (Re (Z)) against the imaginary part of impedance (-Im (Z)). The R_{ct} increased accordingly to TNF-α concentration, confirming that our developed ImmunoFET was sensitive to the raise of TNF-α concentration. The increase in R_{ct} is explained by the binding of TNF-α to the mAb anti-TNF-α immobilized onto the ISFET, which produce an insulating layer that increases the R_{ct}. Then, the Nyquist plots obtained were fitted using the equivalent circuit described in 2.5 and shown in Fig. 1A, and the corresponding fitting parameters are presented in Table 1. Fig. 1B shows the related calibration curve, confirming that our ImmunoFET response is linear to TNF-α concentration, as demonstrated by R^2 equal to 0.988 ± 0.027 (CV% 2%). The calibration curve resulted y = 0.062 (±0.011) x + 0.276 (±0.011). The limit of detection (LOD) of our ImmunoFET was obtained from equation 3 S/m [32], where S is the residual standard deviation of the linear regression and m is the slope of the regression line, and resulted 1 pg mL^{-1}.

3.2. Selectivity study

Selectivity study was carried out by analyzing standard solutions containing TNF-α and three other HF biomarkers namely IL−10, NT-proBNP, and Cortisol in order to assess the levels of interferences from these biomarkers, using the same experimental conditions and concentration range from 5 to 50 pg mL^{-1}. From Fig. 2, our ImmunoFET demonstrate to be highly selective toward TNF-α when compared to the other three HF biomarkers. In fact, the corresponding calibration curves resulted y = 0.060 x + 0.372 (R^2 = 0.993) for TNF-α; y = −0.001 x + 0.357 (R^2 = 0.813) for IL-10; y = −0.002 x + 0.494 (R^2 = 0.701) for NT-proBNP; and y = 0.003 x + 0.196 (R^2 = 0.708) for cortisol.

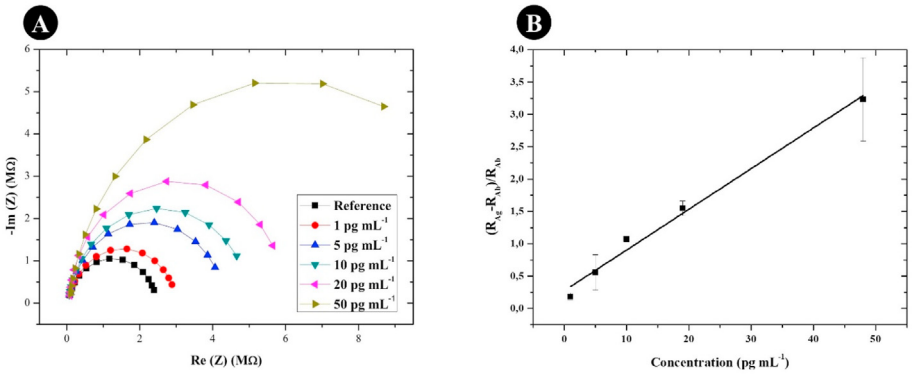

Fig. 1. (A) Example of Nyquist plots (resulted from the fitting of each spectrum to the proposed equivalent circuit) for the equivalent circuit model obtained by analyzing TNF-α standard solutions in PBS (1; 5; 10; 20; and 50 pg mL^{-1}). EIS frequency ranged from 10 kHz to 10 Hz, with E_{ac} 75 mV and E_{dc} 0 V vs Ag/AgCl; **(B)** Calibration curve obtained by analyzing standard solution containing TNF-α in the concentration range 1–50 pg mL^{-1} using the ImmunoFET functionalized with mAb-TNF-α.

Table 1
Fitting parameters obtained from the equivalent circuit model [$R_1 + Q_2/R_2$]. $R_1 = R_S$ is the resistance of the electrolyte solution; Q_2 is the constant phase element; $R_2 = R_{ct}$ is the charge transfer resistance, and χ is the error on the fit.

Concentration	R_1 (kΩ)	Q_2 (nF.s $^{(a-1)}$)	R_2 (kΩ)	χ
Reference	33.270	1.339	2461	7.318 10^{-3}
1 pg mL^{-1}	36.155	1.312	3004	7.431 10^{-3}
5 pg mL^{-1}	39.539	1.098	4316	5.731 10^{-3}
10 pg mL^{-1}	40.171	1.080	5032	4.821 10^{-3}
20 pg mL^{-1}	43.680	1.058	6468	6.216 10^{-3}
50 pg mL^{-1}	45.287	0.9759	11540	3.371 10^{-3}

3.3. Saliva samples

3.3.1. Calibration in saliva sample

Analysis of saliva calibration samples described in 2.4. provided a calibration curve described by y = 0.058 (±0.014) x + 0.144 (±0.130) and confirmed the method linearity by an R^2 equal to 0.995 ± 0.002 (CV 0.2%). The presence of matrix effect was ruled out by comparing the slopes of the calibration curves (i.e. PBS and spiked saliva samples) at a confidence level of 95%. The comparison of calibration curves in PBS and real saliva is shown in Fig. 3.

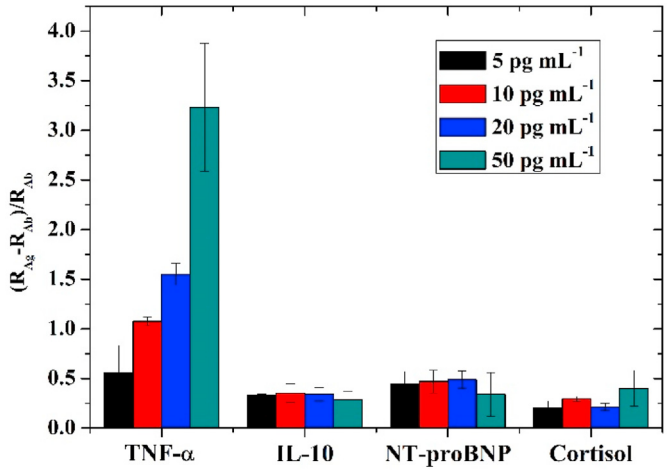

Fig. 2. Results from interference study obtained by analyzing standard solution containing TNF-α or other HF biomarkers (e.g. IL–10, NT-proBNP, and Cortisol) in the concentration range 5–50 pg mL^{-1} using the ImmunoFET functionalized with mAb-TNF-α.

3.3.2. TNF-α quantification in saliva samples by STAM

TNF-α was then quantified in three aliquots of PSS (namely Aliquot I, II, and III, respectively) by performing the standard addition method. As explained in 2.4, Aliquot I was unspiked PSS, whereas Aliquot II and Aliquot III were PSS spiked with TNF-α standard solution obtaining samples containing 50 and 330 pg mL^{-1}, respectively.

The corresponding curves obtained from Aliquot I (which corresponded to unspiked PSS) analysis by performing the STAM resulted linear and described by y = 0.076 (±0.019) x + 0.182 (±0.053), with R^2 = 0.998 (±0.007). According to STAM procedure, the concentration of TNF-α in Aliquot I was extrapolated from the curve by multiplying for the dilution factor of 20 the absolute value on x-axis for y = 0. In this case, TNF-α concentration in Aliquot I resulted in 48 ± 1 pg mL^{-1}. Aliquot II analysis provided a curve described by y = 0.013 (±0.001) x + 0.059 (±0.009) with R^2 = 0.995 (±0.006) and TNF-α concentration resulted 90 ± 11 pg mL^{-1}, whereas Aliquot III analysis provided a curve described by y = 0.013 (±0.002) x + 0.253 (±0.056), with R^2 = 0.987 (±0.007) and, consequently, TNF-α concentration resulted 370 ± 30 pg mL^{-1}.

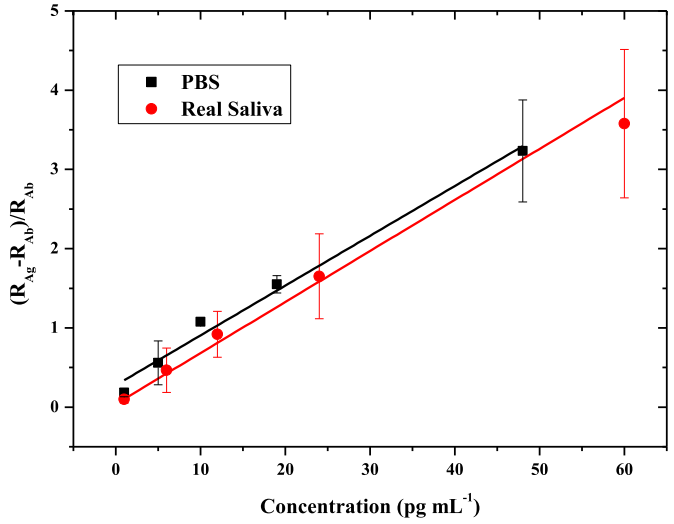

Fig. 3. Comparison of calibration curves used for method linearity and matrix effect investigation that were obtained from the analysis of TNF-α standard solution in PBS (black, described by y = 0.062 (±0.011) x + 0.276 (±0.011) with R^2 = 0.988 ± 0.027) and in spiked saliva samples (red, described by y = 0.058 (±0.014) x + 0.144 (±0.130) with R^2 = 0.995 ± 0.002), respectively. (For interpretation of the references to colour in this figure legend, the reader is referred to the Web version of this article.)

Table 2
Data from saliva sample analysis by performing the STAM to quantify TNF-α.

Sample name	Sample type	Expected TNF-α concentration [pg mL^{-1}]	Calculated TNF-α concentration [pg mL^{-1}]
Aliquot I	Unspiked PSS	Unknown	48 ± 12 pg mL^{-1}
Aliquot II	PSS spiked with 50 pg mL^{-1}	TNF-α concentration in Aliquot I + 50 pg mL^{-1}	90 ± 11 pg mL^{-1}
Aliquot III	PSS spiked with 330 pg mL^{-1}	TNF-α concentration in Aliquot I + 330 pg mL^{-1}	370 ± 30 pg mL^{-1}

Table 2 summarizes the results from analysis of STAM samples. Method precision, here expressed as recovery %, was evaluated by considering the bias between the expected TNF-α concentration and TNF-α calculated by extrapolation from the STAM curve, and resulted 94 ± 6%.

These data (e.g. linearity, selectivity, high precision, and LOD of 1 pg mL^{-1}) allowed considering our ImmunoFET as a very promising tool for monitoring salivary TNF-α concentration and further tests will be carried out and implemented to confirm these results and carry out a pre-clinical study on HF patients.

4. Conclusions

Preliminary results from ImmunoFET analytical validation (e.g. linearity, selectivity, high precision, and LOD of 1 pg mL^{-1}) demonstrated the ability of our ImmunoFET to monitor monitoring salivary TNF-α concentration. Our device also showed high selectivity towards TNF-α when compared to other HF biomarkers such as IL-10, NT-proBNP, and Cortisol. Finally, preliminary tests on TNF-α quantification saliva samples by performing the STAM proved the capacity of our ImmunoFET to determine the TNF-α concentration with a recovery almost quantitative, confirming the satisfying precision of the method. An implementation of a clinical study would fully validate our device. In fact, these results, combined with further improvements in term of accuracy and ImmunoFET integration into a LoC, can allow the monitoring of salivary levels of TNF-α confirming our ImmunoFET as a very promising tool for biomedical application such as HF monitoring by saliva analysis.

CRediT authorship contribution statement

Hamdi Ben Halima: Writing – original draft. **Francesca G. Bellagambi:** Writing – original draft, Formal analysis. **Albert Alcacer:** performed experimental research. **Norman Pfeiffer:** performed experimental research. **Marie Hangouët:** performed experimental research. **Nadia Zine:** Supervision, Project administration, Formal analysis. **Joan Bausells:** Supervision, Project administration, Formal analysis. **Abdelhamid Elaissari:** Supervision, Project administration, Formal analysis. **Abdelhamid Errachid:** Supervision, Project administration, Formal analysis, All authors reviewed and approved the final version of the manuscript.

Declaration of competing interest

The authors declare that they have no known competing financial interests or personal relationships that could have appeared to influence the work reported in this paper.

Acknowledgements

The authors acknowledge the financial support of the European Union's Horizon 2020 research and innovation programme, Project NMBP–13–2017 KardiaTool (Grant agreement No. 768686).

References

[1] E.J. Benjamin, P. Muntner, A. Alonso, M.S. Bittencourt, C.W. Callaway, A.P. Carson, A.M. Chamberlain, A.R. Chang, S. Cheng, S.R. Das, F.N. Delling, L. Djousse, M.S.V. Elkind, J.F. Ferguson, M. Fornage, L. Chaffin Jordan, S.S. Khan, B.M. Kissela, K.L. Knutson, T.W. Kwan, D.T. Lackland, T.T. Lewis, J.H. Lichtman, C.T. Longenecker, M. Shane Loop, P.L. Lutsey, S.S. Martin, K. Matsushita, A.E. Moran, M.E. Mussolino, M. O'Flaherty, A. Pandey, A.M. Perak, W.D. Rosamond, G.A. Roth, U.K.A. Sampson, G.M. Satou, E.B. Schroeder, S.H. Shah, N.L. Spartano, A. Stokes, D.L. Tirschwell, C.W. Tsao, M.P. Turakhia, L.B. VanWagner, J.T. Wilkins, S.S. Wong, S.S. Virani, American heart association council on epidemiology and prevention statistics committee and stroke statistics subcommittee, heart disease and stroke statistics-2019 update: a report from the American heart association, Circulation 139 (2019) e56–e528, https://doi.org/10.1016/j.Sc.2010.00372.

[2] S.S. Virani, A. Alonso, E.J. Benjamin, M.S. Bittencourt, C.W. Callaway, A.P. Carson, A.M. Chamberlain, A.R. Chang, S. Cheng, F.N. Delling, L. Djousse, M.S.V. Elkind, J.F. Ferguson, M. Fornage, S.S. Khan, B.M. Kissela, K.L. Knutson, T.W. Kwan, D.T. Lackland, T.T. Lewis, J.H. Lichtman, C.T. Longenecker, M. Shane Loop, P.L. Lutsey, S.S. Martin, K. Matsushita, A.E. Moran, M.E. Mussolino, A. Marma Perak, W.D. Rosamond, G.A. Roth, U.K.A. Sampson, G.M. Satou, E.B. Schroeder, S.H. Shah, C.M. Shay, N.L. Spartano, A. Stokes, D.L. Tirschwell, L.B. VanWagner, C.W. Tsao, On behalf of the American heart association council on epidemiology and prevention statistics committee and stroke statistics subcommittee, heart disease and stroke statistics—2020 update: a report from the American heart association, Circulation 141 (2020) e139–e596, https://doi.org/10.1161/CIR.0000000000000757.

[3] W. Lesyuk, C. Kriza, P. Kolominsky-Rabas, Cost-of-illness studies in heart failure: a systematic review 2004-2016, BMC Cardiovasc. Disord. 18 (2018) 74, https://doi.org/10.1186/s12872-018-0815-3.

[4] A.A. Shafie, Y.P. Tan, C.H. Ng, Systematic review of economic burden of heart failure, Heart Fail. Rev. 29 (2018) 131–145, https://doi.org/10.1007/s10741-017-9661-0.

[5] A.A. Inamdar, A.C. Inamdar, Heart failure: diagnosis, management and utilization, J. Clin. Med. 5 (2016) 62, https://doi.org/10.3390/jcm5070062.

[6] E.E. Tripoliti, T.G. Papadopoulos, G.S. Karanasiou, K.K. Naka, D.I. Fotiadis, Heart failure: diagnosis, severity estimation and prediction of adverse events through machine learning techniques, Comput. Struct. Biotechnol. J. 15 (2016) 26–47, https://doi.org/10.1016/j.csbj.2016.11.001.

[7] E. Braunwald, Biomarkers in heart failure, N. Engl. J. Med. 358 (2008) 2148–2159, https://doi.org/10.1056/NEJMra0800239.

[8] A. Yndestad, J.K. Damås, E. Øie, E.T. Ueland, L. Gullestad, P. Aukrust, Role of inflammation in the progression of heart failure, Curr. Cardiol. Rep. 9 (2007) 236–241, https://doi.org/10.1007/BF02938356.

[9] L.F. Shirazi, J. Bissett, F. Romeo, J.L. Mehta, Role of inflammation in heart failure, Curr. Atherosclerosis Rep. 19 (2017) 27, https://doi.org/10.1007/s11883-017-0660-3.

[10] C. Riehle, J. Bauersachs, Key inflammatory mechanisms underlying heart failure, Herz 44 (2019) 96–106, https://doi.org/10.1007/s00059-019-4785-8.

[11] J. Holbrook, S. Lara-Reyna, H. Jarosz-Griffiths, M. McDermott, F1000Res, Tumour Necrosis Factor Signalling in Health and Disease, vol. 8, 2019, https://doi.org/10.12688/f1000research.17023.1. F1000 Faculty Rev-111.

[12] M.J. Page, J. Bester, E. Pretorius, The inflammatory effects of TNF-α and complement component 3 on coagulation, Sci. Rep. 8 (2018) 1812, https://doi.org/10.1038/s41598-018-20220-8.

[13] L. Puimège, C. Libert, Van F. Hauwermeiren, Regulation and dysregulation of tumor necrosis factor receptor-1, Cytokine Growth Factor Rev 25 (2014) 285–300, https://doi.org/10.1016/j.cytogfr.2014.03.004.

[14] G. Kleiner, A. Marcuzzi, V. Zanin, L. Monasta, G. Zauli, Cytokine levels in the serum of healthy subjects, Mediat. Inflamm. 2013 (2013) 1–6, https://doi.org/10.1155/2013/434010.

[15] F.G. Bellagambi, T. Lomonaco, P. Salvo, F. Vivaldi, M. Hangouët, S. Ghimenti, D. Biagini, F. Di Francesco, R. Fuoco, A. Errachid, Saliva sampling: methods and devices. An overview, TrAC Trends Anal. Chem. (Reference Ed.) 124 (2020) 115781, https://doi.org/10.1016/j.trac.2019.115781.

[16] S.M. Schumacher, S.V. Naga Prasad, Tumor necrosis factor-α in heart failure: an updated review, Curr. Cardiol. Rep. 20 (2018) 117, https://doi.org/10.1007/s11886-018-1067-7.

[17] O.A. Segiet, A. Piecuch, L. Mielanczyk, M. Michalski, E. Nowalany-kozielska, Role of interleukins in heart failure with reduced ejection fraction, Anatol. J. Cardiol. 22 (2019) 287–299, https://doi.org/10.14744/AnatolJCardiol.2019.32748.

[18] M. Lee, N. Zine, A. Baraket, M. Zabala, F. Campabadal, R. Caruso, M.G. Trivella, N. Jaffrezic-Renault, A. Errachid, A novel biosensor based on hafnium oxide: application for early stage detection of human interleukin-10, Sensor. Actuator. B Chem. 175 (2012) 201–207, https://doi.org/10.1016/j.snb.2012.04.090.

[19] L. Barhoumi, A. Baraket, F.G. Bellagambi, G.S. Karanasiou, M. Ben Ali, D.I. Fotiadis, J. Bausells, N. Zine, M. Sigaud, A. Errachid, A novel chronoamperometric immunosensor for rapid detection of TNF-α in human saliva,

Sensor. Actuator. B Chem. 266 (2018), https://doi.org/10.1016/j.snb.2018.03.135, 477–84.
[20] L. Barhoumi, A. Baraket, F.G. Bellagambi, F.M. Vivaldi, A. Baraket, Y. Clément, N. Zine, M. Ben Ali, A. Elaissari, A. Errachid, Ultrasensitive immunosensor array for TNF-α detection in artificial saliva using polymer-coated magnetic microparticles onto screen-printed gold electrode, Sensors 19 (2019) E692, https://doi.org/10.3390/s19030692.
[21] P. Gümüş, N. Nizam, D.F. Lappin, N. Buduneli, Saliva and serum levels of B-cell activating factors and tumor necrosis factor-α in patients with periodontitis, J. Periodontol. 85 (2014) 270−280, https://doi.org/10.1902/jop.2013.130117.
[22] A. Longo, A. Baraket, M. Vatteroni, N. Zine, J. Baussells, RogerFuoco, F. Di Francesco, G.S. Karanasiou, D.I. Fotiadis, A. Menciassi, A. Errachid, Highly sensitive electrochemical BioMEMS for TNF-α detection in human saliva: heart Failure, Procedia Eng 168 (2016) 97−100, https://doi.org/10.1016/j.proeng.2016.11.156.
[23] F.G. Bellagambi, I. Degano, S. Ghimenti, T. Lomonaco, V. Dini, M. Romanelli, F. Mastorci, A. Gemignani, P. Salvo, R. Fuoco, F. Di Francesco, Determination of salivary α-amylase and cortisol in psoriatic subjects undergoing the Trier Social Stress Test, Microchem. J. 136 (2018) 177−184, https://doi.org/10.1016/j.microc.2017.04.033.
[24] S. Ghimenti, T. Lomonaco, F.G. Bellagambi, D. Biagini, P. Salvo, M.G. Trivella, M.C. Scali, V. Barletta, M. Marzilli, F. Di Francesco, A. Errachid, R. Fuoco, Salivary lactate and 8-isoprostaglandin $F_{2\alpha}$ as potential non-invasive biomarkers for monitoring heart failure: a pilot study, Sci. Rep. 10 (2020) 7441, https://doi.org/10.1038/s41598-020-64112-2.
[25] D. Biagini, T. Lomonaco, S. Ghimenti, J. Fusi, E. Cerri, F. De Angelis, F.G. Bellagambi, C. Oger, J.M. Galano, E. Bramanti, F. Franzoni, R. Fuoco, F. Di Francesco, Saliva as a non-invasive tool for monitoring oxidative stress in swimmers athletes performing a VO_{2max} cycle ergometer test, Talanta 216 (2020) 120979, https://doi.org/10.1016/j.talanta.2020.120979.
[26] F.G. Bellagambi, A. Baraket, A. Longo, M. Vatteroni, N. Zine, J. Bausells, R. Fuoco, F. Di Francesco, P. Salvo, G.S. Karanasiou, D.I. Fotiadis, A. Menciassi, A. Errachid, Electrochemical biosensor platform for TNF-α cytokines detection in both artificial and human saliva: heart failure, Sensor. Actuator. B Chem. 251 (2017) 1026−1033, https://doi.org/10.1016/j.snb.2017.05.169.
[27] D. Vozgirdaite, H. Ben Halima, F.G. Bellagambi, A. Alcacer, F. Palacio, N. Zine, J. Bausells, A. Errachid, Development of an ImmunoFET for the detection of TNF-α in saliva: application to heart failure monitoring, Chemosensors 9 (2021) 26, https://doi.org/10.3390/chemosensors9020026.
[28] D. Caballero, J. Samitier, J. Bausells, A. Errachid, Direct patterning of anti-human serum albumin antibodies on aldehyde-terminated silicon nitride surfaces for HSA protein detection, Small 5 (2009) 1531−1534, https://doi.org/10.1002/smll.200801735.
[29] H. Ben Halima, N. Zine, J. Gallardo-Gonzalez, A.E. Aissari, M. Sigaud, A. Alcacer, J. Bausells, A. Errachid, A novel cortisol biosensor based on the capacitive structure of hafnium oxide: application for heart failure monitoring, in: 2019 20th International Conference on Solid-State Sensors, Actuators and Microsystems & Eurosensors XXXIII (TRANSDUCERS & EUROSENSORS XXXIII), IEEE, Berlin, Germany, 2019, pp. 1067−1070, https://doi.org/10.1109/TRANSDUCERS.2019.8808561.
[30] T. Lomonaco, S. Ghimenti, D. Biagini, E. Bramanti, M. Onor, F.G. Bellagambi, R. Fuoco, F. Di Francesco, The effect of sampling procedures on the urate and lactate concentration in oral fluid, Microchem. J. 136 (2018) 255−262, https://doi.org/10.1016/j.microc.2017.02.032.
[31] D. Biagini, S. Antoni, T. Lomonaco, S. Ghimenti, P. Salvo, F.G. Bellagambi, R.T. Scaramuzzo, M. Ciantelli, A. Cuttano, R. Fuoco, F. Di Francesco, F, Microextraction by packed sorbent combined with UHPLC-ESI-MS/MS for the determination of prostanoids and isoprostanoids in dried blood spots, Talanta 206 (2020) 120236, https://doi.org/10.1016/j.talanta.2019.120236.
[32] A. Shrivastava, V. Gupta, Methods for the determination of limit of detection and limit of quantitation of the analytical methods, Chronicles Young Sci. 2 (2011) 21, https://doi.org/10.4103/2229-5186.79345.